

Selected Paper

Semiquantal Valence-Bond Wave Packet Description of Chemical Bonding

Koji Ando

Department of Chemistry, Graduate School of Science, Kyoto University, Kyoto 606-8502

Received March 10, 2009; E-mail: ando@kuchem.kyoto-u.ac.jp

A semiquantal wave packet modeling of electrons in chemical bonding is presented. It is based on the valence bond (VB) theory with non-orthogonal floating and breathing spherical Gaussian orbitals, simplified to treat many electrons by decoupled electron pair approximations (DPA) and core pseudopotentials (CPP). The extended Hamiltonian formalism offers pictorial interpretation and analysis in the extended phase space of the wave packet center and width coordinates. The numerical calculations are demonstrated on the ground state potential energy surfaces of H_2, LiH, and BeH_2. For LiH, the perfect-pairing VB (VB-PP) calculation with the minimal orbitals gives an accurate potential energy curve of comparable quality with a correlated ab initio calculation. The two-electron VB calculation with a CPP underestimates the binding energy but gives qualitatively correct potential energy curves. For BeH_2, the VB-PP with CPP gives reasonably accurate potential energy surface along both the stretching and bending coordinates. A few versions of DPA are developed and assessed, aiming toward large scale dynamic simulations. A scaling ansatz is introduced and examined on the bonding potential energy surfaces. The efficacy of the theory for studying linear and nonlinear electronic polarizations is also illustrated via an analysis of potential energy surfaces in the extended phase space.

A goal of theoretical and computational chemistry is to develop approaches to the solution of full molecular time-dependent Schrödinger equations treating both electronic and nuclear degrees of freedom as dynamical variables. This is obviously too demanding for chemical problems involving both degrees of freedom in non-trivial manners. A range of approximations and models are therefore deployed. One end is represented by high-level ab initio quantum chemical calculations with large scale electron-correlation methods;[1,2] the other is statistical mechanical simulations by molecular dynamics (MD), Monte Carlo, and integral-equation methods.[3,4] The former are yet too expensive for the direct dynamic simulations of large systems, while the latter often employ simplified potential functions ignoring electronic structure alterations.

The hybrid of these two ends, the so-called QM/MM strategy, has been a major arena in the last decade.[5,6] Nonetheless, consistent treatment of the boundary between QM (quantum mechanics) and MM (molecular mechanics) regions has been the bottleneck both technically and conceptually. Another growing area is the simulation of real-time electron dynamics by time-dependent Hartree–Fock, time-dependent density functional, and other methods.[7–10] These are naturally more expensive than their time-independent counterparts.

While qualifying the promise of these state-of-the-art computations,[11] in this work we investigate a different approach. It is motivated by the recent development of semiquantal time-dependent Hartree (SQTDH) theory for chemical dynamics in condensed phase.[12–14] The SQTDH theory describes the wave function as a Hartree product of the squeezed coherent state Gaussian wave packets. The structure and dynamics of the wave function can be studied in a pictorial manner on a potential surface in an extended phase space formed by the wave packet center and width coordinates. This has been demonstrated for coupled system-bath models[12] and hydrogen-bonding structures.[13]

As the Hartree approximation implies however, many-fermion systems were out of the scope of the SQTDH theory. We therefore attempt in this work to extend it to account for the antisymmetry of electronic wave functions. To this end, we exploit and combine the ideas of the valence bond (VB) theory, non-orthogonal floating and breathing orbitals, decoupled electron pair approximation (DPA), and core pseudopotentials (CPP). It is thus designed to achieve semiquantitative correctness and applicability to large scale dynamic simulations.

The time-independent electronic part of the present theory is partially related to the FSGO (floating spherical Gaussian orbital) method.[15] The main difference is the restricted Hartree–Fock (RHF) nature of the latter, contrasted with the VB idea of the former. On the other hand, the dynamic part is related to the fermion wave packet MD simulations in nuclear and plasma physics.[16–20] The distinction is in the treatment of the antisymmetry of the wave function and the DPA based on the VB coupling, reflected in the form of the Pauli potential. The present work shares the motivation with the eFF (electron force field) model by Su and Goddard,[21] although the formulation and the resultant potential function are different.

In this first report, the basic framework of the theory is described and numerical applications are examined on the ground state potential energy surfaces of small molecules such as H_2, LiH, and BeH_2. Applications to larger systems and to dynamic processes will be presented in forthcoming publications.

Published on the web August 7, 2009; doi:10.1246/bcsj.82.975

Next section describes the theory for one and two electron systems, a scaling ansatz, and the CPP and DPA for many electron systems. The third section presents numerical applications and discussions. The paper concludes in the fourth sction.

Theory

One Electron Atoms and Molecules. Basic Framework: For simplicity, we set $\hbar = 1$ and assume that the coordinates are mass-scaled. The trial wave function[22–24] is defined in the coherent state spherical Gaussian form,

$$\phi(\boldsymbol{q}, t) = N \exp\{A(t)|\boldsymbol{q} - \boldsymbol{x}(t)|^2 + i\boldsymbol{p}(t) \cdot (\boldsymbol{q} - \boldsymbol{x}(t))\} \tag{1}$$

in which

$$A(t) = \frac{-1 + 2i\rho(t)\pi(t)}{4\rho(t)^2} \tag{2}$$

and $N = (2\pi\rho(t)^2)^{-\frac{3}{4}}$ is the normalization factor. The time-dependent parameters $\boldsymbol{x}(t)$ and $\rho(t)$ describe the center and width of the wave packet; $\boldsymbol{p}(t)$ and $\pi(t)$ are seen below to represent the conjugate momenta of $\boldsymbol{x}(t)$ and $\rho(t)$.

The equations of motion for the parameters are derived from the time-dependent variational theory,[25] $\delta(\int L\mathrm{d}t)/\delta X = 0$, where X represents all the parameters, and

$$L = \langle\phi(t)|i\frac{\partial}{\partial t} - \hat{H}|\phi(t)\rangle \tag{3}$$

with $\hat{H} = -(1/2)\partial^2/\partial q^2 + V(q)$. This yields

$$\begin{aligned} \dot{\boldsymbol{x}} &= \partial H_{\mathrm{ext}}/\partial \boldsymbol{p}, \quad \dot{\boldsymbol{p}} = -\partial H_{\mathrm{ext}}/\partial \boldsymbol{x} \\ \dot{\rho} &= \partial H_{\mathrm{ext}}/\partial \pi, \quad \dot{\pi} = -\partial H_{\mathrm{ext}}/\partial \rho \end{aligned} \tag{4}$$

in which H_{ext} is given by

$$H_{\mathrm{ext}} = \frac{\boldsymbol{p}^2}{2} + \frac{\pi^2}{2} + \frac{3}{8\rho^2} + \langle V\rangle \tag{5}$$

where $\langle V\rangle$ is the expectation value of V with respect to $|\phi\rangle$. The classical Hamiltonian form of eq 4 suggests consideration of the phase space $(\boldsymbol{x}, \rho, \boldsymbol{p}, \pi)$. The key quantity is therefore the potential

$$V_{\mathrm{ext}} = \frac{3\hbar^2}{8m\rho^2} + \langle V\rangle \tag{6}$$

in the extended configuration space $(\boldsymbol{x}, \rho)$. Note that $\hbar$ and the mass m are retrieved in the first term of eq 6. This term tends to broaden the wave packet, with a stronger tendency when the mass is lighter, and vanishes in the classical limit $\hbar \to 0$. The optimal stationary state wave packet in the ground state is obtained simply by minimizing V_{ext}.

In Ref. 24, the problem of constructing an extended potential for coupled degrees of freedom has been pointed out. The Hartree ansatz was examined in Ref. 12 together with the canonicity condition (Ref. 26) for the extended Hamiltonian form. It was found to be essentitally equivalent to the QHD-2 (quantized Hamilton dynamics)[27] and QCD (quantized cumulant dynamics)[28] theories by assuming decoupling of the degrees of freedom. In this work, the use of the spherical Gaussian form evades this problem for the three Cartesian coordinates of a particle. It also obviates the issue concerning the rotational invariance.

Hydrogen-Like Atoms: The theory is well illustrated on the hydrogen-like atoms. Hereafter, we apply the atomic unit $\hbar = e = m_e = 1$. The potential for the electron at position $\boldsymbol{q}$ is

$$V_{\mathrm{H}}(\boldsymbol{q}) = -Z/|\boldsymbol{q}| \tag{7}$$

where the nucleus with atomic number Z is placed at the origin. In this work, we treat the nucleus as a classical point charge (the Born–Oppenheimer approximation). The wave packet treatment of nuclei will be treated elsewhere.

The semiquantal extended potential is derived straightforwardly as

$$V_{\mathrm{H}}^{\mathrm{ext}}(\boldsymbol{x}, \rho) = \frac{3}{8\rho^2} - \sqrt{\frac{2}{\pi}}\frac{Z}{\rho}F_0\left(\frac{|\boldsymbol{x}|^2}{2\rho^2}\right) \tag{8}$$

in which F_0 is the Boys function[29] of order 0 defined by

$$F_0(t) = \int_0^1 e^{-ty^2}\mathrm{d}y = \sqrt{\frac{\pi}{4t}}\,\mathrm{erf}(\sqrt{t}) \tag{9}$$

The minimum of $V_{\mathrm{H}}^{\mathrm{ext}}$ is found at $\boldsymbol{x} = 0$ from the symmetry. Therefore, $V_{\mathrm{H}}^{\mathrm{ext}}$ is a quadratic function of $1/\rho$ whose minimum is at

$$\rho = \frac{3}{4Z}\sqrt{\frac{2}{\pi}}\ (\equiv \rho_0) \tag{10}$$

which is 0.940 bohr for $Z = 1$. The minimum energy is

$$V_{\mathrm{H}}^{\mathrm{ext}}(0, \rho_0) = -\frac{4Z^2}{3\pi} \tag{11}$$

which is ca. 85% of the exact 1s energy $E_{\mathrm{H}} = -Z^2/2$. The same result has been found in Ref. 30. Here we will extend the analysis to the scaling ansatz and the calculation of polarizability. A note on the virial theorem is included in Appendix.

Static Polarizability: The polarizability is calculated from the energy change induced by an electric field $\boldsymbol{F}$, which adds a field-electron interaction $-\boldsymbol{F}\cdot\boldsymbol{q}$ to the Hamiltonian. The numerical calculation is straightforward, and the effect is pictured as a deformation of the extended potential V_{ext}, as will be demonstrated later. The analytical solution is available for the hydrogen-like atoms, which is described below.

Let us assume that a uniform field is applied along the z axis. As the static polarizability is defined in the weak field limit, we expand the Boys function in eq 8 around $\boldsymbol{x} = 0$,

$$V_{\mathrm{H}}^{\mathrm{ext}}(z, \rho; F) \simeq \frac{3}{8\rho^2} - \sqrt{\frac{2}{\pi}}\frac{Z}{\rho}\left(1 - \frac{z^2}{6\rho^2}\right) - Fz \tag{12}$$

Minimizing along z,

$$V_{\mathrm{H}}^{\mathrm{ext}}(z_0, \rho; F) = V_{\mathrm{H}}^{\mathrm{ext}}(0, \rho; 0) - \frac{3}{2Z}\sqrt{\frac{\pi}{2}}\rho^3F^2 \tag{13}$$

where $z_0 = (3/Z)\sqrt{\pi/2}\rho^3F$. The polarizability α is thus

$$\alpha = \frac{3}{Z}\sqrt{\frac{\pi}{2}}\rho_0^3 = \frac{81\pi^2}{256Z^4} \approx 3.12/Z^4 \tag{14}$$

which is ca. 69% of the value 9/2 from the perturbation theory[31] for the hydrogen atom.

Scaling Ansatz: The underestimate of the energy for the hydrogen-like atoms in eq 11 stems from the use of the Gaussian function. This is related to the cusp condition satisfied by the exact 1s function but not by the Gaussian function.[32] Nonetheless, we may explore scaling properties when the theory is consistent within the variational subspace.

Table 1 compares the expectation values of some powers of the electron–nucleus radial distance r from the exact and the semiquantal theories for the ground state of the hydrogen-like atoms. As seen in eq 11, the energy is scaled as

$$E_{\mathrm{H}}^{\mathrm{SQ}} = \frac{8}{3\pi}E_{\mathrm{H}}^{\mathrm{exact}} \tag{15}$$

Table 1. Expectation Values of Some Powers of the Electron–Nucleus Radial Distance r for the Ground State Hydrogen-Like Atoms[a)]

	Exact	Semiquantal	Using ρ_0
$\langle r \rangle$	$\frac{3}{2}a$	$\sqrt{\frac{8}{\pi}}\tilde{\rho}$	$\frac{3}{2}a$
$\langle r^2 \rangle$	$3a^2$	$3\tilde{\rho}^2$	$\frac{27\pi}{32}a^2$
$\langle r^{-1} \rangle$	a^{-1}	$\sqrt{\frac{2}{\pi}}\tilde{\rho}^{-1}$	$\frac{8}{3\pi}a^{-1}$
$\langle r^{-2} \rangle$	$2a^{-2}$	$\tilde{\rho}^{-2}$	$\frac{32}{9\pi}a^{-2}$

a) $a \equiv a_0/Z$ where a_0 is the Bohr radius and Z is the atomic number. $\tilde{\rho} \equiv \rho/Z$ and ρ_0 is from eq 10.

This suggests that we introduce a scaling correction factor

$$\gamma_E \equiv \frac{3\pi}{8} \tag{16}$$

for energies computed from the semiquantal theory.

For the length scale, a possible factor is suggested from the ratio of $\langle r \rangle$,

$$\gamma'_L = \frac{\langle r \rangle_{\text{exact}}}{\langle r \rangle_{\text{SQ}}} = 1 \tag{17}$$

Another possibility would be to refer to $\langle r^{-1} \rangle$,

$$\gamma''_L = \frac{\langle r^{-1} \rangle_{\text{SQ}}}{\langle r^{-1} \rangle_{\text{exact}}} = \frac{8}{3\pi} \tag{18}$$

Since the arithmetic and geometric means of γ'_L and γ''_L give similar numbers, 0.924 and 0.921, we choose the latter for simplicity,

$$\gamma_L \equiv \sqrt{\gamma'_L \gamma''_L} = \sqrt{\frac{8}{3\pi}} \tag{19}$$

These scaling corrections will be carried over and examined on chemical bondings in the third section.

Two Electron Atoms and Molecules. Here we summarize the Heitler–London[33] (HL) VB framework. The main purpose is to fix the notations. The HL-VB wave function for two electrons is

$$\psi^{\text{HL}}_{ab}(1,2) = \frac{1}{\sqrt{2(1+S^2_{ab})}}(\phi_a(\boldsymbol{q}_1)\phi_b(\boldsymbol{q}_2) + \phi_b(\boldsymbol{q}_1)\phi_a(\boldsymbol{q}_2)) \times \frac{1}{\sqrt{2}}(\alpha(1)\beta(2) - \beta(2)\alpha(1)) \tag{20}$$

As we restrict the numerical calculations to the stationary wave functions in this work, the momentum parameters $\boldsymbol{p}$ and π in eq 1 are nullified and the spatial orbitals $\phi_a(\boldsymbol{q})$ are specified by the wave packet center $\boldsymbol{x}_a$ and width ρ_a. α and β are the spin functions. S_{ab} is the overlap integral between ϕ_a and ϕ_b.

The corresponding electronic energy is given by

$$E^{\text{HL}}_{ab} = \frac{1}{1+S^2_{ab}}(h_{aa} + h_{bb} + 2S_{ab}h_{ab} + (aa|bb) + (ab|ab)) \tag{21}$$

where h_{ab} is the one-electron integral consisting of the kinetic energy and the electron–nuclear potential. $(aa|bb)$ and $(ab|ab)$ are the two-electron Coulomb and exchange integrals. These integrals are summarized in Appendix.

Many Electron Systems and DPA. As is well-known, the complexity of the non-orthogonal VB calculation grows rapidly along with the number of electrons. It is thus essential to devise efficient approximations in order to realize large scale simulations. In this section, we develop and examine a few versions of DPA. To this end, it is useful to work on four electron systems for which the VB treatment is still handy (with $4! = 24$ matrix elements).

In the first approximation, we show that the VB energy can be simplified to a pairwise form by rearranging the energy expression and introducing the Mulliken approximation[34] to the integrals. This is further simplified to a form that contains terms resembling the so-called Pauli potential.[16–18] In the third approximation, the wave function is completely decoupled to a product of the HL-VB pair functions.

VB Energy for Four Electrons: The energy of the perfect-pairing VB (VB-PP) wave function[35] in which orbital pairs (a,b) and (c,d) are coupled in the singlet configuration is given by[36]

$$E^{\text{VBPP}}_{ab\cdot cd} = \frac{1}{\Delta}(Q + J_2 + J_3 + J_4) \tag{22}$$

where

$$Q = \sum_a h_{aa} + \sum_{a<b}(aa|bb) \tag{23}$$

and J_n ($n = 2$, 3, and 4) represents n-electron exchange integrals. For example, J_2 is given by

$$J_2 \equiv J_{ab} + J_{cd} - (J_{ac} + J_{ad} + J_{bc} + J_{bd})/2 \tag{24}$$

where

$$\begin{aligned} J_{ab} &\equiv \langle abcd|H|bacd\rangle \\ &= 2h_{ab}S_{ab} + (h_{cc} + h_{dd})S^2_{ab} + (ab|ba) \\ &\quad + 2\{(ab|cc) + (ab|dd)\}S_{ab} + (cc|dd)S^2_{ab} \end{aligned} \tag{25}$$

The normalization factor is given by

$$\Delta = 1 + S^2_{ab} + S^2_{cd} - (S^2_{ac} + S^2_{ad} + S^2_{bc} + S^2_{bd})/2 + S_3 + S_4 \tag{26}$$

The formulas for the third- and fourth-order exchange and overlap integrals J_3, J_4, S_3, and S_4 are rather lengthy, for which we would refer to Ref. 36.

The two-electron part of Q is the Coulomb interaction between electron distributions $|\phi_a|^2$ and $|\phi_b|^2$. The calculation of the pairwise interactions of this sort is already the bottleneck in large scale simulations. In this sense, the three- and four-center integrals such as $(ab|cc)$ and $(ab|cd)$ in J_n ($n = 2$, 3, and 4) will impose additional and higher computational demands. We shall thus seek for approximations to reduce the energy to simpler forms.

DPA-1: Integral Approximation to the VB Energy: In the first approximation, we neglect the higher order terms J_3, J_4, S_3, and S_4 and rewrite J_2 in eq 22 as

$$\begin{aligned} E^{\text{VBPP}}_{ab\cdot cd} &\simeq \frac{1}{\Delta}(Q + J_2) \\ &= Q - \frac{1}{\Delta}[S^2_{ab}j_{ab} + S^2_{cd}j_{cd} \\ &\quad - (S^2_{ac}j_{ac} + S^2_{ad}j_{ad} + S^2_{bc}j_{bc} + S^2_{bd}j_{bd})/2] \end{aligned} \tag{27}$$

where

$$j_{ab} \equiv Q - J_{ab}/S^2_{ab} \tag{28}$$

This still contains the three-center integrals in J_{ab}. Nonetheless, by applying the Mulliken approximation,[34]

$$(ab|cd) \simeq (S_{ab}/2)(S_{cd}/2) \times [(aa|cc) + (aa|dd) + (bb|cc) + (bb|dd)] \tag{29}$$

we find j_{ab} reduces to a pairwise quantity of ϕ_a and ϕ_b,

$$j_{ab} \simeq h_{aa} + h_{bb} - 2h_{ab}/S_{ab} + (aa|bb) - (ab|ba)/S_{ab}^2 \quad (30)$$

The use of eqs 27 and 30 will be called DPA-1.

Pauli Potential Form (DPA-2): We may further approximate the denominator Δ in eq 27 to decouple into

$$E_{ab\cdot cd}^{\mathrm{DPA2}} = Q - \frac{S_{ab}^2}{1+S_{ab}^2} j_{ab} - \frac{S_{cd}^2}{1+S_{cd}^2} j_{cd} + \frac{S_{ac}^2/2}{1-S_{ac}^2/2} j_{ac} + \frac{S_{ad}^2/2}{1-S_{ad}^2/2} j_{ad} + \frac{S_{bc}^2/2}{1-S_{bc}^2/2} j_{bc} + \frac{S_{bd}^2/2}{1-S_{bd}^2/2} j_{bd} \quad (31)$$

which will be called DPA-2. The last four terms have a form similar to the Pauli potential,[16–18] but with the extra factor $1/2$ to the overlap integrals. This factor reflects the spin couplings between the electrons in different pairs; the spins in orbitals ϕ_a and ϕ_c may be either parallel or anti-parallel, e.g., $\alpha\beta\cdot\alpha\beta$ or $\alpha\beta\cdot\beta\alpha$, in $ab\cdot cd$. In contrast, the factor $1/2$ is absent in the previous Pauli potentials, as they are derived from the triplet (parallel) spin coupling.

DPA-3: Decoupled Product Wave Function: In the third approximation, we decouple the wave function into the product form

$$\psi(1,2,3,4) \simeq \psi_{ab}^{\mathrm{HL}}(1,2)\psi_{cd}^{\mathrm{HL}}(3,4) \quad (32)$$

The energy of this wave function consists of the HL-VB energies of the ab and cd pairs of the form eq 21 and the interaction between them. The latter contains the three- and four-center integrals. Introducing the Mulliken approximation and j_{ab} of eq 30, however, the energy is again reduced to a pairwise form,

$$E_{ab\cdot cd}^{\mathrm{DPA3}} = Q - \frac{S_{ab}^2}{1+S_{ab}^2} j_{ab} - \frac{S_{cd}^2}{1+S_{cd}^2} j_{cd} \quad (33)$$

which will be called DPA-3. This coincides with the first three terms in the right hand side of eq 31, although the derivations are different as we have seen. The energy formulas appear to suggest that DPA-2 is an intermediate between DPA-1 and DPA-3. This will be examined numerically in the third section.

Pseudopotentials for Core Electrons. We will see in the third section that the VB-PP energy of eq 22 gives a good description of the core-valence interaction. Nonetheless, CPPs will be useful for large scale simulations.

In this work, we employ a CPP of the form

$$V_{\mathrm{cpp}}(r) = -\frac{Z-Z_c}{r}(1 - A_c \exp(-r^2/4\rho_c^2)) \quad (34)$$

where Z_c is the number of core electrons. The parameter ρ_c represents the width of the potential. This potential is Coulombic in the large r region, but its behavior at $r = 0$ is singular at $A_c = 1$; $V_{\mathrm{cpp}}(0)$ vanishes for $A_c = 1$, but diverges to $\pm\infty$ for $A_c > 1$ and $A_c < 1$.

In the calculations in the third section, we only use $A_c = 1$ for simplicity. This choice follows the previous studies[37–39]—although their functional forms are designed for use with the plane wave basis—that anticipate cancellation of kinetic and potential energies in the core region. In this regard, eq 34 with $A_c = 1$ is distinguished from the ECP (effective core potential) popular in quantum chemistry.

With $A_c = 1$, we need one parameter ρ_c per element. Nonetheless, considering the dependence $\rho_0 \propto Z^{-1}$ in eq 10, we may seek a common parameter $\tilde{\rho}_c$ to scale as $\rho_c = \tilde{\rho}_c/Z$ for elements in a row in the periodic table.

Results and Discussion

In this work, the energy minimization was carried out by the Brent's method[40] that does not require derivatives.

Hydrogen Molecule. The importance of orbital breathing in the covalent bonding of H_2 has been known for a long time.[41] The effect of orbital floating was studied with both the VB and the MO-CI (molecular orbital-configuration interaction) methods, and was concluded to be minor.[30,42,43] Then, presumably due to the historical prevalence of the MO-CI methods, the orbital floating seems to have been paid less attention in the VB compared to the MO-CI.[44–48] Here, we briefly revisit the problem within the present framework, aiming to set up a groundwork for the later sections.

Figure 1a shows the potential energy curves of H_2 from various calculations. It is seen that the energy and length scalings discussed in the previous section shift the curve closer to the accurate calculation by Kolos and Wolniewicz.[49] The equilibrium bond length is 1.557 and 1.435 bohr before and after the scaling, compared to 1.4011 bohr by Kolos–Wolniewicz.

For comparison, the RHF and unrestricted Hartree–Fock (UHF) calculations are included. The RHF scheme corresponds to the FSGO method.[15] We also examined the mixing of an ionic VB function

$$\frac{1}{\sqrt{2(1+S_{ab}^2)}}(\phi_a\phi_a + \phi_b\phi_b)(\alpha\beta - \beta\alpha)/\sqrt{2} \quad (35)$$

In this case, the wave packet centers are fixed at the nuclear positions, which would be in accord with the idea of the "ionic" function. The mixing coefficients of the covalent and ionic components are fully optimized. This is thus equivalent to the full CI in the minimal breathing basis. As seen in the figure, the mixing of the ionic component lowers the energy particularly in the region of longer internuclear distance.

The effects of orbital floating and breathing and of the ionic function are compared in Figure 1b. It is seen that both the orbital floating and the ionic component lower the energy but do not change much the equilibrium bond length. In contrast, the orbital breathing notably lowers the energy and shortens the equilibrium bond length.

LiH: Assessment of VB-PP and CPP. Figure 2 shows the potential energy curves of LiH from the four-electron VB-PP and the HL-VB with use of the CPP. For comparison, the Morse function derived from the experimental spectroscopic constants[50,51] and the MRMP2 (multi-reference second-order Møller–Plesset perturbation) calculation[52] with the cc-pVDZ basis set are included. We used the program GAMESS[53] for the MRMP2 calculation. In the CASSCF (complete active space self-consistent field) calculation prior to the MRMP2, the 1s core orbital of Li was frozen and two electrons were distributed in the six valence orbitals.

As seen in the figure, the VB-PP calculation gives the result close and parallel to the MRMP2 and the experimental Morse potentials. This is remarkable for the compactness of the wave function formed by one floating and breathing orbital per electron. The result also indicates that the present VB-PP wave function is free from the problem in describing the core–valence interaction pointed out in the FSGO method.[54,55]

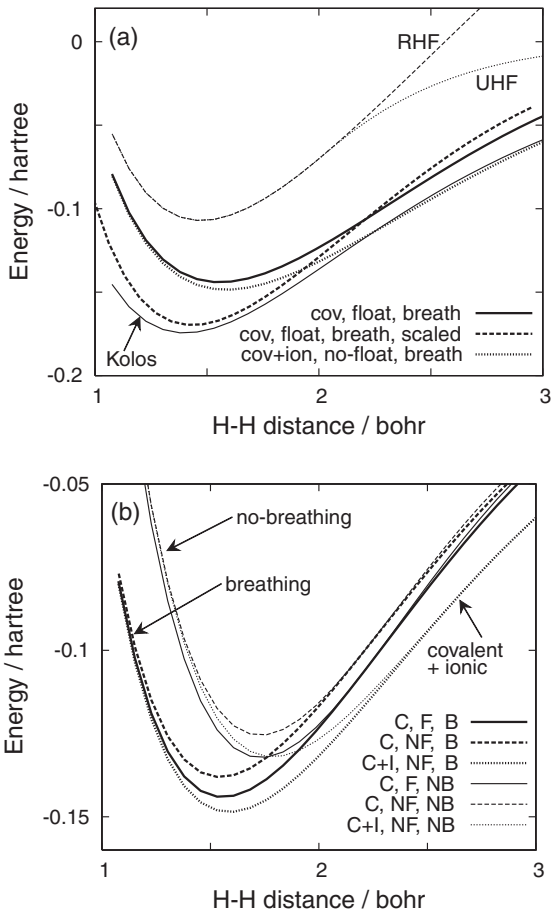

Figure 1. Potential energy curves of hydrogen molecule. (a) Thick solid: covalent VB with floating and breathing orbitals (SQ-HLVB). Thick dashed: SQ-HLVB with the energy and length scalings. Thick dotted: covalent + ionic VB, no-floating but breathing. Thin solid: Kolos–Wolniewicz. Thin dashed: RHF, floating and breathing. Thin dotted: UHF, floating and breathing. (b) Thick solid: covalent only (C), floating (F), and breathing (B). Thick dashed: covalent only, no-floating (NF) but breathing. Thick dotted: covalent + ionic (C+I), no-floating but breathing. Thin solid: covalent only, floating but no-breathing (NB). Thin dashed: covalent only, no-floating and no-breathing. Thin dotted: covalent + ionic, no-floating and no-breathing.

To the VB-PP calculation shown in the figure, we did not apply the energy and length scalings, but the equilibrium bond length is already close to the accurate references. This seems to imply that the screening by the 1s core electrons is effective such that the error due to the lack of wave function cusp is masked for the valence electron, in contrast with the case of H_2 (See also Figure 3 discussed below.).

In the calculation with CPP, we searched the optimal value of the parameter ρ_c with an increment of 0.1 bohr and found that $\rho_c = 0.7$ bohr gives the thick dashed curve in the figure. In general, the smaller ρ_c yields the shorter equilibrium bond length. Therefore, we also examined slightly larger $\rho_c = 0.8$ bohr combined with the scaling ansatz, as displayed by the thick dotted curve. As seen, these two calculations give similar

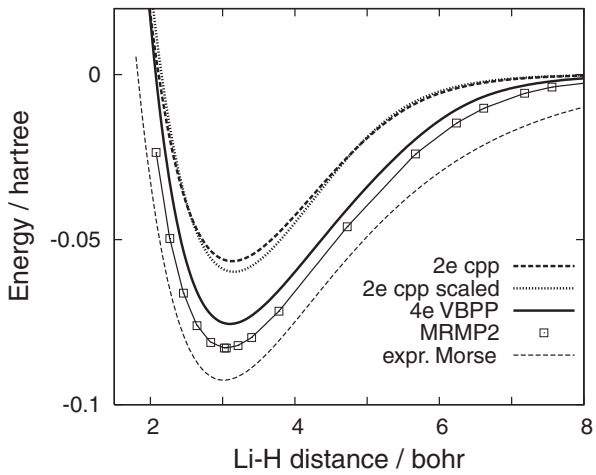

Figure 2. Potential energy curves of LiH. Thick solid: Four electron SQ-VBPP. Thick dashed: Two electron SQ-HLVB with CPP of $\rho_c = 0.7$ bohr. Thick dotted: Two electron scaled SQ-HLVB with CPP of $\rho_c = 0.8$ bohr. Box marks: MRMP2/cc-pVDZ. Thin dotted: Morse function from experimental spectroscopic constants.

results that are both reasonably parallel to the MRMP2 and the experimental Morse potentials. The underestimate of the binding energy is seemingly due to the use of CPP.

Figure 3 displays the wave packet widths (a) and the center positions (b). The latter are measured from the Li nucleus. The nearly constant lines in (a) at $\rho = 0.25$ and 0.50 bohr represent the Li 1s core electrons in the VB-PP calculation. These are centered at the Li nucleus as seen in (b). The remaining two orbitals represent the valence electrons assigned to Li and H. Both shrink as the atoms approach to each other, indicating the increase of the kinetic energy associated with the bond formation. This is in accord with the virial theorem (see also the section: Extended Potential Surfacce). In the region of Li–H distance longer than 5 bohr, the solid and dashed curves for the width of Li valence orbital start to deviate notably. In the same region, the orbital center starts to move from the internuclear region toward the Li nucleus. The deviation thus comes from the different descriptions of the core–valence interaction. For the H orbital, the two calculations give similar width in the entire bond length region, and the orbital center stays close to the proton nucleus.

BeH_2: Assessment of DPAs. Figure 4 shows the potential energy curves of BeH_2 along the Be–H symmetric stretch distance and the H–Be–H bending angle. The three versions of DPA and VB-PP are compared against MRMP2. A CPP with $\rho_c = 0.6$ bohr is used for the 1s core of Be. This ρ_c is related via $\rho_c = \tilde{\rho}_c/Z$ to the $\rho_c = 0.8$ bohr for Li in the previous section.

As noted before, the underestimate of the binding energy seems to come from the use of CPP. Similarly to the cases of H_2 and LiH, the scaling prescription improves the results, but the curves shown in the figure are the unscaled ones.

In the previous section, we have noted that the energy formula for DPA-2 appears to be the intermediate between DPA-1 and DPA-3. This simple view is, however, not supported by the results in Figure 4. The shapes of the

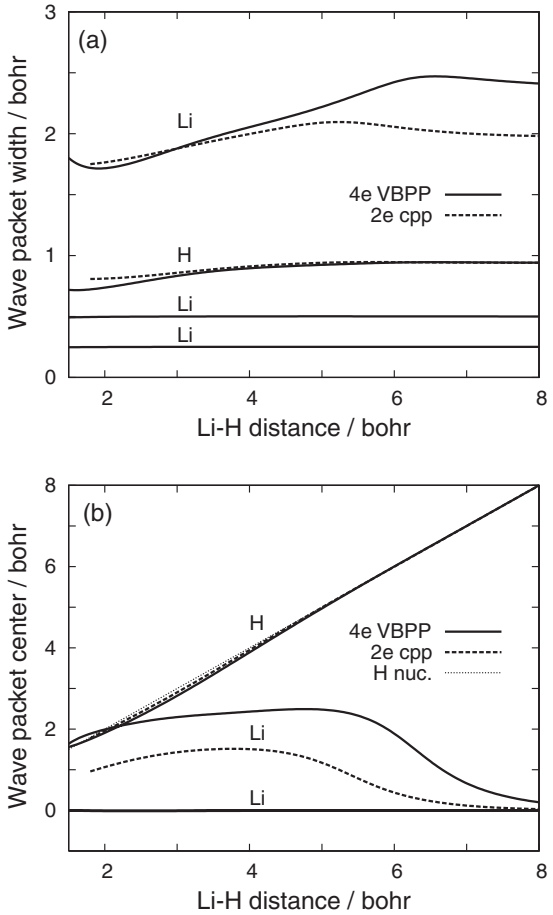

Figure 3. Wave packet parameters for LiH. (a) Wave packet widths. (b) Wave packet centers measured from the Li nucleus. Solid: Four electron SQ-VBPP. Dashed: Two electron SQ-HLVB with CPP of $\rho_c = 0.7$ bohr. In (b), the dotted line denotes the position of the proton.

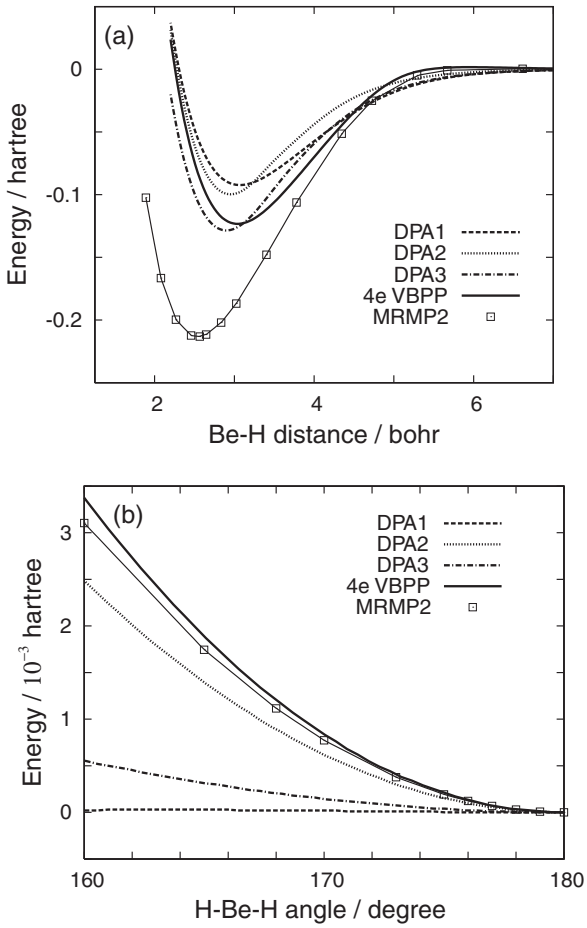

Figure 4. Potential energy curves of BeH_2. (a) Along the symmetric stretch of the BeH distance. (b) Along the H–Be–H angle at $r(\mathrm{BeH}) = 2.566$ bohr. Solid: Four electron SQ-VBPP. Dashed: DPA-1. Dotted: DPA-2. Dash-dotted: DPA-3. Box marks: MRMP2/cc-pVDZ.

potential look similar between VB-PP and DPA-1 and between DPA-2 and DPA-3.

Regarding the bending potential, VB-PP is closest to the MRMP2 reference, and DPA-2 comes next. The success of DPA-2 is presumably due to some cancellation of errors. To clarify this, we have checked the wave packet center and width parameters, but could not draw a definite conclusion. Further investigation is needed on this issue, along with the extension to larger systems.

Extended Potential Surface. Figure 5 shows the deformation of the extended potential energy surface $V_{\mathrm{H}}^{\mathrm{ext}}(r, \rho)$ (eq 8 with $r = |\boldsymbol{x}|$) of a hydrogen atom under a uniform static electric field. In Figure 5b with $F = 0.08$ au, the minimum energy point is located at $r = 0.293$ bohr and $\rho = 0.983$ bohr, the latter being larger than the $\rho_0 = 0.940$ bohr of eq 10. The energy change from the isolated atom is computed to be -0.01077 hartree, which is larger in magnitude than that calculated from the polarizability of eq 14, $-\alpha F^2/2 = -0.00999$ hartree. This reflects the nonlinearity of the polarization under this strong field.

The extended potential energy surfaces for the electrons in H_2 are displayed in Figure 6. The position of the electron wave packet center x is measured from the center of the two nuclei and along the H–H bond. Figures 6a and 6b are calculated at the H–H distance $R = 1.4$ and 2.5 bohr, compared to the equilibrium bond length $R = 1.557$ bohr obtained in the previous section.

The corresponding parameters and energies are listed in Table 2, together with the quantities pertaining to the virial theorem. As the H–H bond is stretched, the wave packet centers of the electrons move closer to the nuclear position, and the wave packet widths become larger. The virial theorem is satisfied at the equilibrium bond length, as expected for the fully optimized floating and breathing orbitals. The change of the virial ratio $-\langle V\rangle/\langle T\rangle$ implies that the raise of the energy in the shorter bond length is due to the increase of the kinetic energy, which is connected to the behavior of the wave packet width ρ (See also the discussion around Figure 3.).

For general many electron systems, the adiabatic elimination of uninteresting degrees of freedom will be useful, similarly to that demonstrated for the system-bath models.[12] The dynamic polarization can be studied by the Hamiltonian trajectory on the extended potential surface within the present framework. These extensive subjects will be treated in separate publications.

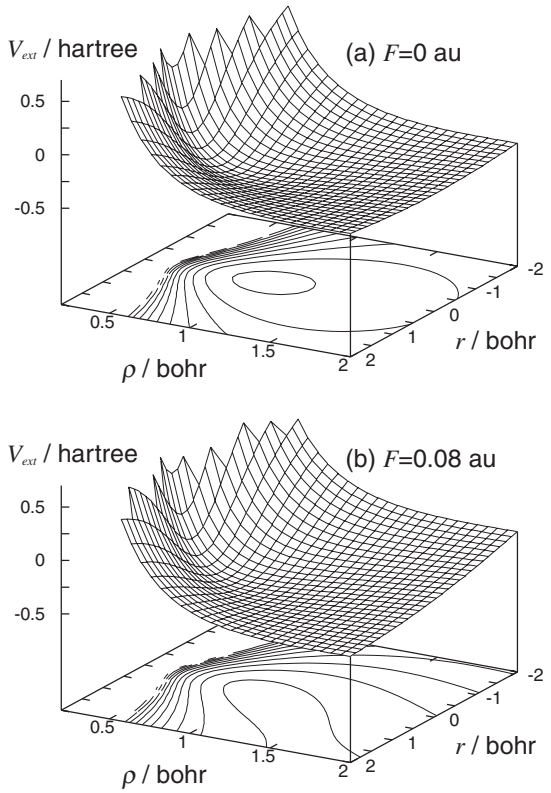

Figure 5. Extended potential $V_{\text{ext}}(r, \rho)$ for hydrogen atom. (a) Isolated atom. (b) Under electric field $F = 0.08$ au.

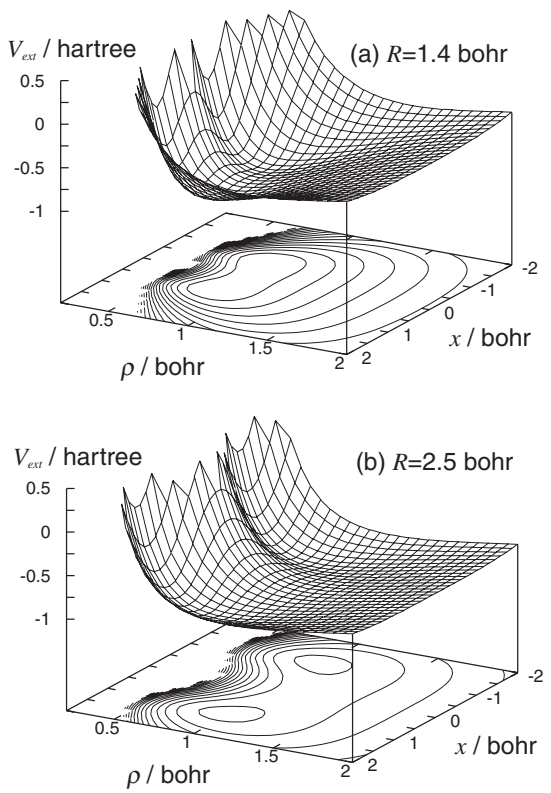

Figure 6. Extended potential $V_{\text{ext}}(x, \rho)$ for hydrogen molecule. (a) The H–H distance $R = 1.4$ bohr. (b) $R = 2.5$ bohr.

Table 2. Results from the SQ-HLVB Calculation on Hydrogen Molecule[a)]

R	x	Δx	ρ	E	$-\langle V\rangle/\langle T\rangle$	$\langle V\rangle/2E$
1.4	0.600	0.100	0.805	−0.9882	1.91569	1.04603
1.557	0.668	0.111	0.837	−0.9929	2.00002	0.99999
2.5	1.135	0.116	0.971	−0.9303	2.28857	0.88803

a) $\Delta x \equiv R/2 - x$ is the shift of the wave packet center from the nuclei. Lengths in bohr, energy in hartree.

Concluding Remarks

A study on the semiquantal wave packet modeling of electrons in chemical bonding has been presented. In contrast with the traditional MO picture based on the delocalized single-particle mean-field approximation, the VB framework fits well with the localized electron wave packet ansatz. The floating and breathing spherical Gaussian orbitals are found to give the potential energy surfaces of reasonable accuracy with the minimal number of orbitals. Emerging is thus not simply the localized orbital picture but the corpuscular picture of the electrons.

On developing the DPA and CPP, our motivation was promoted by the empirical success of the VSEPR (valence shell electron pair repulsion) theory.[56] Although the VB-PP result on LiH is encouraging, the examinations of the DPAs and CPP indicates that further analysis and development are needed for extension to larger systems. Since the orbitals are inherently localized in the present framework, we may, for example, include the higher order terms in the VB energy only for locally adjacent pairs.

Other directions in which to proceed will be toward dynamic simulations and the semiquantal treatment of protons and other light nuclei. The latter is related to the nuclear-orbital methods,[57–59] which are more elaborate and hence intriguing to compare. Work on these extensions will be reported in forthcoming publications.

Appendix

Integral Formulas. Here we compile the formulas for the energy integrals. The one-electron integrals consist of the kinetic and electron-nuclear terms,

$$h_{ab} = T_{ab} + V_{ab}^{\text{ne}} \tag{36}$$

where

$$T_{ab} = \frac{1}{4(\rho_a^2 + \rho_b^2)}\left(3 - \frac{|\boldsymbol{x}_a - \boldsymbol{x}_b|^2}{2(\rho_a^2 + \rho_b^2)}\right)S_{ab} \tag{37}$$

with the overlap integral

$$S_{ab} = \left(\frac{2\rho_a\rho_b}{\rho_a^2 + \rho_b^2}\right)^{\frac{3}{2}} \exp\left(-\frac{|\boldsymbol{x}_a - \boldsymbol{x}_b|^2}{4(\rho_a^2 + \rho_b^2)}\right) \tag{38}$$

and

$$\begin{aligned} V_{ab}^{\text{ne}} &= \langle\phi_a(\boldsymbol{q})|\sum_I -\frac{Z_I}{|\boldsymbol{q} - \boldsymbol{R}_I|}|\phi_b(\boldsymbol{q})\rangle \\ &= -\left(\frac{\rho_a^2 + \rho_b^2}{\pi\rho_a^2\rho_b^2}\right)^{\frac{1}{2}} S_{ab}\sum_I Z_I F_0\left(\frac{\rho_a^2 + \rho_b^2}{4\rho_a^2\rho_b^2}|\boldsymbol{x}_p - \boldsymbol{R}_I|^2\right) \end{aligned} \tag{39}$$

in which $\boldsymbol{R}_I$ and Z_I denote the nuclear coordinates and the atomic numbers. $\boldsymbol{x}_p$ is the center of the product $\phi_a\phi_b$ defined by

$$\boldsymbol{x}_p = \frac{\rho_b^2 \boldsymbol{x}_a + \rho_a^2 \boldsymbol{x}_b}{\rho_a^2 + \rho_b^2} \tag{40}$$

The two-electron Coulomb and exchange integrals are calculated from

$$(aa|bb) = \left(\frac{2}{\pi(\rho_a^2 + \rho_b^2)}\right)^{\frac{1}{2}} F_0\left(\frac{|\boldsymbol{x}_a - \boldsymbol{x}_b|^2}{2(\rho_a^2 + \rho_b^2)}\right) \tag{41}$$

and

$$(ab|ab) = \left(\frac{\rho_a^2 + \rho_b^2}{2\pi\rho_a^2\rho_b^2}\right) S_{ab}^2 \tag{42}$$

The above formulas will be sufficient to fix the notations and to compare with the previous fermion MD methods. For the three- and four-center two-electron integrals, use of the general formula[60] and the conversion between the Gaussian exponents and the width parameters ρ is convenient.

Virial Theorem for Hydrogen-Like Atoms. For stationary wave functions, we may regard the first term of eq 8 as the kinetic energy part, which is denoted by T. With the variationally optimized $\boldsymbol{x} = 0$ and $\rho = \rho_0$ of eq 10 for the hydrogen-like atoms, we find

$$\langle T \rangle = \frac{3}{8\rho_0^2} = \frac{4Z^2}{3\pi} \tag{43}$$

and

$$\langle V \rangle = -\sqrt{\frac{2}{\pi}}\frac{Z}{\rho_0} = -\frac{8Z^2}{3\pi} \tag{44}$$

Therefore, the virial theorem for Coulomb systems

$$2\langle T \rangle + \langle V \rangle = 0 \tag{45}$$

is satisfied. The virial theorem for H_2 is examined in the section: Extended Potential Surface.

This work has been supported by KAKENHI in Priority Areas "Molecular Theory for Real Systems" (No. 190296) and "Emergence of Highly Elaborated π-space and its Function" (No. 20106017).

References

1 *Recent Advances in Multireference Methods*, ed. by K. Hirao, World Scientific, Singapore, **1999**.
2 T. Helgaker, P. Jørgensen, J. Olsen, *Molecular Electronic-Structure Theory*, Wiley, Chichester, **2000**.
3 M. P. Allen, D. J. Tidesley, *Computer Simulation of Liquids*, Clarendon, Oxford, **1987**.
4 *Molecular Theory of Solvation*, ed. by F. Hirata, Kluwer Academic, Dordrecht, **2003**.
5 K. Yasuda, D. Yamaki, *J. Chem. Phys.* **2004**, *121*, 3964.
6 H. Lin, D. G. Truhlar, *Theor. Chem. Acc.* **2007**, *117*, 185.
7 H. B. Schlegel, S. M. Smith, X. Li, *J. Chem. Phys.* **2007**, *126*, 244110.
8 K. Burke, J. Werschnik, E. K. U. Gross, *J. Chem. Phys.* **2005**, *123*, 062206.
9 T. Kato, H. Kono, *J. Chem. Phys.* **2008**, *128*, 184102.
10 T. Yonehara, K. Takatsuka, *J. Chem. Phys.* **2008**, *128*, 154104.
11 We apologize that the reference list in the above is far from complete.
12 K. Ando, *J. Chem. Phys.* **2004**, *121*, 7136.
13 K. Ando, *J. Chem. Phys.* **2006**, *125*, 014104.
14 N. Sakumichi, K. Ando, *J. Chem. Phys.* **2008**, *128*, 164516.
15 A. A. Frost, in *Modern Theoretical Chemistry*, Vol. 3, ed. by H. F. Shaefer, Plenum, New York, **1977**.
16 L. Wilets, E. M. Henley, M. Kraft, A. D. Mackellar, *Nucl. Phys.* **1977**, *A282*, 341.
17 C. Dorso, S. Duarte, J. Randrup, *Phys. Lett. B* **1987**, *188*, 287.
18 D. Klakow, C. Toepffer, P.-G. Reinhard, *J. Chem. Phys.* **1994**, *101*, 10766.
19 A. Ono, H. Horiuchi, T. Maruyama, A. Ohnishi, *Prog. Theor. Phys.* **1992**, *87*, 1185.
20 H. Feldmeier, J. Schnack, *Rev. Mod. Phys.* **2000**, *72*, 655.
21 J. T. Su, W. A. Goddard, *Proc. Natl. Acad. Sci. U.S.A.* **2009**, *106*, 1001.
22 This form of the trial function in one-dimension has been studied in Refs. 23 and 24, and called a "semiquantal" ansatz in the latter. The semiquantal and semiclassical theories were distinguished as the classical nature emerges by restricting the Hilbert space in the former, while the classical trajectories are approximately quantized in the latter.
23 F. Arickx, J. Broeckhove, E. Kesteloot, L. Lathouwers, P. van Leuven, *Chem. Phys. Lett.* **1986**, *128*, 310.
24 A. K. Pattanayak, W. C. Schieve, *Phys. Rev. E* **1994**, *50*, 3601.
25 P. Kramer, M. Saraceno, *Geometry of the Time-Dependent Variational Principle in Quantum Mechanics*, Springer, Berlin, **1981**.
26 T. Marumori, T. Maskawa, F. Sakata, A. Kuriyama, *Prog. Theor. Phys.* **1980**, *64*, 1294.
27 O. V. Prezhdo, *Theor. Chem. Acc.* **2006**, *116*, 206.
28 Y. Shigeta, H. Miyachi, T. Matsui, K. Hirao, *Bull. Chem. Soc. Jpn.* **2008**, *81,* 1230.
29 S. F. Boys, *Proc. Roy. Soc. Lond. A* **1950**, *200*, 542.
30 C. M. Reeves, *J. Chem. Phys.* **1963**, *39*, 1.
31 L. Pauling, E. B. Wilson, *Introduction to Quantum Mechanics with Applications to Chemistry*, Dover, New York, **1985**.
32 The Slater-type exponential functions are, however, not adequate for the floating basis as they introduce unnecessary cusps in the free space between the nuclei.
33 W. Heitler, F. London, *Z. Phys.* **1927**, *44*, 455.
34 R. S. Mulliken, *J. Chim. Phys.* **1949**, *46,* 500; R. S. Mulliken, *J. Chim. Phys.* **1949**, *46,* 521.
35 Here we deal with a single VB configuration consisting of the perfect-pairing spin-couplings such as $\alpha\beta{\cdot}\alpha\beta$ and three others, and not with the resonance between the alternative spin-coupling configuration such as $\alpha\alpha{\cdot}\beta\beta$. Cases where the resonance is essential will be discussed elsewhere.
36 J. C. Slater, *Phys. Rev.* **1931**, *38*, 1109.
37 M. H. Cohen, V. Heine, *Phys. Rev.* **1961**, *122*, 1821.
38 N. W. Ashcroft, *Phys. Lett.* **1966**, *23*, 48.
39 W. C. Topp, J. J. Hopfield, *Phys. Rev. B* **1973**, *7*, 1295.
40 R. Brent, *Algorithms for Minimization without Derivatives*, Dover, New York, **2002**.
41 S. C. Wang, *Phys. Rev.* **1928**, *31*, 579.
42 H. Shull, D. D. Ebbing, *J. Chem. Phys.* **1958**, *28*, 866.
43 A. C. Hurley, *Proc. Roy. Soc. Lond. A* **1954**, *226*, 179.
44 H. Nakatsuji, S. Kanayama, S. Harada, T. Yonezawa, *J. Am. Chem. Soc.* **1978**, *100*, 7528.
45 H. Huber, *THEOCHEM* **1981**, *76*, 277.
46 T. Helgaker, J. Almlöf, *J. Chem. Phys.* **1988**, *89*, 4889.

47 K. Hirao, K. Mogi, *J. Comput. Chem.* **1992**, *13*, 457.
48 M. Tachikawa, K. Taneda, K. Mori, *Int. J. Quantum Chem.* **1999**, *75*, 497.
49 W. Kolos, L. Wolniewicz, *J. Chem. Phys.* **1968**, *49*, 404.
50 F. H. Crawford, T. Jorgensen, Jr., *Phys. Rev.* **1935**, *47*, 932.
51 W. Meyer, P. Rosmus, *J. Chem. Phys.* **1975**, *63*, 2356.
52 K. Hirao, *Chem. Phys. Lett.* **1992**, *190*, 374.
53 M. W. Schmidt, K. K. Baldridge, J. A. Boatz, S. T. Elbert, M. S. Gordon, J. H. Jensen, S. Koseki, N. Matsunaga, K. A. Nguyen, S. J. Su, T. L. Windus, M. Dupuis, J. A. Montgomery, Jr., *J. Comput. Chem.* **1993**, *14*, 1347.
54 B. Ford, G. G. Hall, J. C. Packer, *Int. J. Quantum Chem.* **1970**, *4*, 533.
55 To quote from Ref. 54, "...a single Gaussian is such a poor representation of the cusp, (...), that an outer function will try to move on to the nucleus to improve the representation there rather than to remain outside and represent the more weakly bound electrons.
56 R. J. Gillespie, E. A. Robinson, *Angew. Chem., Int. Ed. Engl.* **1996**, *35*, 495.
57 H. Nakai, *Int. J. Quantum Chem.* **2007**, *107*, 2849.
58 T. Ishimoto, M. Tachikawa, U. Nagashima, *J. Chem. Phys.* **2008**, *128*, 164118.
59 A. Chakraborty, S. Hammes-Schiffer, *J. Chem. Phys.* **2008**, *129*, 204101.
60 A. Szabo, N. S. Ostlund, *Modern Quantum Chemistry*, Dover, New York, **1996**.